Measurement 156 (2020) 107534

Contents lists available at ScienceDirect

Measurement

journal homepage: www.elsevier.com/locate/measurement

Traffic congestion monitoring using an improved kNN strategy

Fouzi Harrou [a,*], Abdelhafid Zeroual [b,c,d], Ying Sun [a]

[a] Computer, Electrical and Mathematical Sciences and Engineering (CEMSE) Division, King Abdullah University of Science and Technology (KAUST), Thuwal 23955-6900, Saudi Arabia
[b] Faculty of technology, University of 20 August 1955, Skikda 21000, Algeria
[c] LAIG Laboratory, University of 08 May 1945, Guelma 24000, Algeria
[d] CReSTiC URCA UFR SEN, University of Reims Champagne-Ardenne, Moulin de la Housse, France

ARTICLE INFO

Article history:
Received 18 August 2019
Received in revised form 2 January 2020
Accepted 20 January 2020
Available online 25 January 2020

Keywords:
Traffic congestion
Kalman filter
k-Nearest neighbors
Traffic management
Anomaly detection

ABSTRACT

A systematic approach for monitoring road traffic congestion is developed to improve safety and traffic management. To achieve this purpose, an improved observer merging the benefits of a piecewise switched linear traffic (PWSL) modeling approach and Kalman filter (KF) is introduced. The PWSL-KF observer is utilized as a virtual sensor to emulate the traffic evolution in free-flow mode. In the proposed approach, residuals from the PWSL-KF model are used as the input to k-nearest neighbors (kNN) schemes for congestion detection. Here, kNN-based Shewhart and exponential smoothing schemes are designed for discovering the traffic congestions. The proposed detectors merge the desirable properties of kNN to appropriately separating normal from abnormal features and the capability of the monitoring schemes to better identify traffic congestions. In addition, kernel density estimation has been utilized to set non-parametric control limits of the proposed detectors and compared them with their parametric counterparts. Tests on traffic measurements from the four-lane State Route 60 in California freeways show the effectiveness of the PWSL-KF-based kNN methods in supervising traffic congestions.

1. Introduction

Road traffic congestion is increasing significantly over recent decades by the continuous development of countries and the increasing need of road transportation [1]. Accordingly, traffic monitoring and supervision becomes important to handle congestions and provide pertinent information to avoid accidents [2,3]. Indeed, traffic data abundance is a key element that can be used for testing and implementing monitoring approaches. Several traffic detectors using a variety of technologies have been designed and developed for traffic monitoring [4,5]. These detectors include inductive loops, magnetic radio frequency, video microwave infrared and global positioning system.

In general, traffic detectors can be classified in two main groups [6]: sensor-based and vision-based monitoring approach. Vision-based techniques use features obtained from images usually acquired vias cameras. For instance, recently in [7], a novel smart camera sensing that is part of an Internet of things (IoT) system is designed to monitor traffic flow in a smart city. The aim of this smart system is monitoring the traffic flow by detecting and tracking vehicles, people and bicycles. This smart system is tested in the Australian city of Liverpool with 20 smart visual sensors. In [8], a traffic monitoring approach is introduced based on the analysis of videos of the inspected road. This approach is performed in two complementary steps: 1) the detection and counting of vehicles, and 2) generation of the needed information that will be used for managing the traffic. To this end, Haar-like features are extracted from videos and used by the Adaboost algorithm for vehicle detection. Then, the number of vehicles are determined using two virtual detection lines. Finally, the road condition is classified within four classes: free-flow, moderate, busy and heavy traffic. In [9], a vision-based approach is proposed for robust real-time monitoring by applying a deep learning-based detector for vehicle detection, an integrated Discriminative Correlation Filter and a Kalman filter for tracking, and Hungarian algorithm for the data association to extract relevant information of the previous steps. Other works used stereovision-based deep learning methods, such as deep stacked autoencoder (DSA) and deep belief networks (DBNs), for obstacle detection in autonomous vehicles [10,11]. These methods use deep learning models to extract important information from stereovision images and apply a binary clustering algorithm for uncovering obstacles in road environments. Recently, in [12], unmanned aerial vehicles (UAVs) are used with artificial intelligence for traffic monitoring. Specifically, the convolutional neural network algorithm is applied to images collected via UAVs for uncovering traffic congestion.

* Corresponding author.
E-mail address: fouzi.harrou@kaust.edu.sa (F. Harrou).

https://doi.org/10.1016/j.measurement.2020.107534
0263-2241/

However, vision-based methods require image processing, which is time-consuming [13]. Furthermore, long shadows linking vehicles together and transition between day and night are major drawbacks of video monitoring systems. On another hand, the sensor-based monitoring approach uses magnetic loop detectors that permit an accurate counting of vehicles and stability of data collection in different traffic conditions [14]. In [15] monitoring sensor-based approach is proposed using multiple data sources and applying Single-Constraint-At-A-Time (SCAAT) Kalman filters for fusing data and estimation. In [16] discrete-time Markov chain sensor-based monitoring approach is introduced to predict the probability of traffic congestion and identify the freeway bottlenecks. The method in [17] used a hybrid model that merges both vision and sensors based monitoring. Essentially, it is a based model control that monitors the congestion by controlling the clearance of lanes and the function of real-time traffic density. Recently, in [18] a new traffic monitoring approach is proposed using mobile devices. Three algorithms are used in the implementation of this approach: map-matching for location correction, virtual inductive loop for estimation and traffic data collector algorithm. Indeed, the loop detectors are still dominating the installations traffic detectors due to their commodity-priced compared to the other detectors. Also, sensors measurements are used for traffic monitoring without any preprocessing [19,20]. However, continuously collecting traffic data requires the implementation of sensors, which are expensive in terms of implementation and maintenance.

Thereby, traffic state estimation permits providing data using reduced magnetic loop detectors, it comes as virtual sensors and promising solutions for traffic monitoring. Model-based estimation one of powerful technologies that permit providing measurements through virtual sensors [21]. It based essentially on the model that describes traffic dynamics and using estimation methodologies [22]. The estimation based model approaches prove its ability to provide estimations in real-time as well as its facility in implementation and accuracy one time the model describes well the dynamics. Herein, the based traffic model is the PWSL model, proposed recently in [23]. It is a macroscopic model that permits to give a realistic description of traffic phenomena through its nature of the hybrid system. The PWSL has the advantage of the less computation time and high flexibility in the description of traffic dynamics for various road sections lengths.

The first contribution of this paper is designing a model-based traffic estimation approach by integrating the benefits of Kalman filter (KF) and the PWSL model. The proposed PWSL-KF approach is a model-based observer that exploits the suitable performance of KF estimation and the realistic and the flexibility of the PWSL traffic model for reconstructing and estimating traffic state like traffic density. This approach permits estimating the traffic state and used as a virtual sensor that emulates traffic flow evolution.

All over the years, Kalman filters have been widely used in state estimations and modeling tasks. They are suitable tools for estimating and imputing missed data based on a reduced amount of information [24]. Thus, several applications and extensions of the Kalman filter are proposed in the literature. For instance, in [25] an extended Kalman filter introduced together with the fuzzy system to design the adaptive fuzzy strong taking Kalman filter and used to improve the tracking capability of the Global Positioning System in high dynamic environments. In [26], the Kalman filter has been introduced and used as a spectral abundance estimator in spectral characterization, which is important for features and target detection and estimation. In [27], a mechanism merging Kalman filter and χ^2 detector has been used to uncover attacks targeting power grid sensors. This approach used the Kalman filter for emulating the functioning of the grid's sensors under anomaly-free conditions. In [28], A sensor fusion framework using a Kalman filter, which gives robustness to system parameters uncertainties and state initialization, is proposed. In this paper, the Kalman filter is used for road traffic estimation. Then, it will be used with PWLS to generate residuals for traffic monitoring and congestion detection.

Traffic congestion monitoring is key to ensuring sustainable traffic management and improving safety and comfort of driving. Accordingly, a systematic detection of traffic congestion is primordial to improve safety and traffic management. The contributions of this paper are threefold.

- Firstly, an integrated PWSL with Kalman Filter has been designed using a free-flow traffic data. The developed PWSL-KF observer merges the suitable characteristics of PWSL and KF. In fact, the PWSL-KF observer plays the role of a virtual sensor by emulating the real sensors operating in normal conditions. Here, the residuals representing the mismatch between the output of the PWSL-KF observer and the output of the real sensors are used as an indicator of traffic congestion. When the traffic measurements are free-flow, the residuals produced would be around zero. On the other hand, if there is traffic congestion, the residuals would importantly depart from zero. The processing of the residuals using statistical detectors provides an indication of the presence of potential congestion.
- Secondly, a framework integrating k-nearest neighbors (kNN) scheme and univariate monitoring methods (Shewhart and exponential smoothing (ES) charts) is proposed for congestion detection. Then, kNN-based schemes are used to evaluate residuals for sensing potential congestion. Importantly, the key concept of the kNN algorithm, which is an unsupervised detector, for traffic congestion detection is to evaluate the dissimilarity between the new testing data and the free-flow (training) data. This algorithm requires only free-flow in training without any data labeling and it has shown remarkable success in handling nonlinear features.
- Additionally, kernel density estimation is used to compute nonparametrically the detection limits of the proposed kNN-based congestion detection schemes and compared with their parametric counterparts.

The feasibility of the designed strategy is evaluated using traffic measurements gathered from the four-lane SR-60 freeway in southern California. Results show that the proposed strategy can efficiently sense traffic congestions.

The studied road section and data acquisition are presented in Section 2. Then, the proposed PWSL-KF estimator is introduced in Section 3. In Section 4, the designed kNN-based detectors (parametric and nonparametric) and their application in traffic congestion monitoring are described. Section 4.4 presents the developed PWSL-KF-based kNN approaches. Section 5 presents the experimental results and discussions. Lastly, Section 6 concludes this study.

2. Data acquisition and studied road section

Traffic measurements with high precision are vital in the development of efficient traffic control and management systems. Magnetic loop detectors are one of the most used in traffic detection systems to manage traffic congestion. They are still used because of their stability under different lighting and traffic conditions. In inductive loops, the loop induction decreased once the vehicle passing on the embedded circuit, which permits detecting vehicles, counting traffic and monitoring the speed of vehicles (Figure 1).

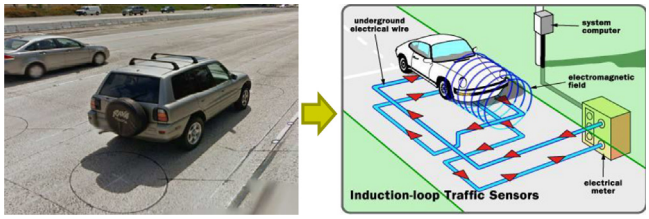

Fig. 1. Illustration of loop detection system.

Here, traffic density and speed are gathered via magnetic loop detectors, which is then employed to control traffic congestion.

In this study, a four lanes road section from SR60 Highway of the state of California highways is considered. A 1.73 miles road section, which is bounded by San Antonio and San Grove avenues, is selected to validate and test the proposed methodology. The considered road section is equipped with VDSs (Vehicles Detection Stations) that permit the collection of traffic measurements. The selected road section is divided into four cells of 0.43 miles, every cell comprises a VDS (Fig. 2). The sensors used in VDSs on the SR60 for traffic monitoring are inductive loop traffic detectors [29]. Each detection station contains an embedded loop circuit in the ground, loop card, and communication system that permit collecting and sharing data (Figure 1).

3. The PWSL-KF design for traffic state estimation

3.1. PWSL approach

Numerous modeling methodologies are developed to model traffic dynamics in the last few decades. The cell transmission (CTM) modeling [30], which is one of the frequently utilized in the literature, is considered as a discretized and simplified version of the first order macroscopic model [31]. It models the traffic flow dynamics by discretizing the Lighthill Whitham Richards(LWR) model spatially (on cells i of length δx_i) and temporary (on step time δT). The occupancy dynamic $n_i(k)$ is given as following:

$$n_i(k+1) = n_i(k) + \Delta T\big(q_i(k) - q_{i+1}(k)\big). \tag{1}$$

The traffic flow $q_i(k)$ can be computed through the min function between the supply occupancy $(n_{i-1}(k))$, the demand one $(\frac{w_i}{v_{f,i}}(n_j - n_i(k)))$ and the maximum flow $Q_{M,i}$:

$$q_i(k) = min\left(n_{i-1}(k), Q_{M,i}, \frac{w_i}{v_{f,i}}\left(n_{j,i} - n_i(k)\right)\right), \tag{2}$$

where $n_{j,i}$ is the maximum occupancy, v_f is the free flow speed and w is the congestion flow speed.

Recently, to accurately describe traffic dynamics, a new hybrid approach called the Piecewise Switched linear macroscopic traffic model (PWSL) [23] has been developed as an enhanced CTM version. This model is based on the notion of the congestion wave propagation and switch between a set of modes, within each mode, it gives different dynamics of traffic flow according to the wave congestion propagation [23]. For enhancing the expression of traffic dynamic, the PWSL use the density dynamics instead of occupancy as in the conventional CTM version. The density dynamics in each cell i is:

$$\rho_i(k+1) = \rho_i(k) + \frac{\Delta T}{\Delta x_i}\left(q_{i,in}(k) - q_{i,out}(k)\right). \tag{3}$$

The PWSL model in each mode is given as,

$$\rho(k+1) = A_s\rho(k) + B_s u(k) + D_s, \tag{4}$$

$$D_s = B_{jam,s}\rho_j + B_{Q,s}Q_M, \tag{5}$$

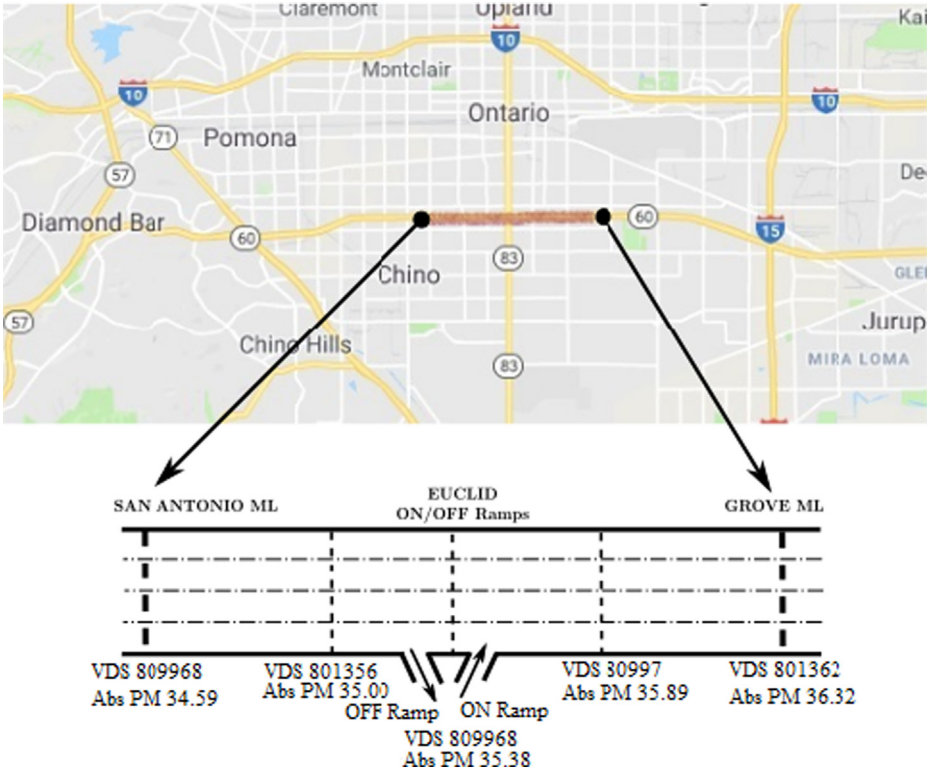

Fig. 2. Geographic location of the SR 60 freeway.

Table 1
PWSL parameters signification.

Parameter	Signification
$s = \{1, \ldots, 2N\}$	Mode system index
$\rho(k) = [\rho_1(k), \ldots, \rho_N(k)]^T$	Density state vector
$u(k) = [q_{in}(k), q_{ON,2}(k), \ldots, q_{ON,N-1}(k), q_{out}(k)]^T$	Entering flow vector contains ramps flow
$\rho_j = [\rho_{j,1}, \ldots, \rho_{j,N}]$	Jam density vector
$y(k)$	System output
$A_s \in \mathbb{R}^{N\times N}, B_s \in \mathbb{R}^{N\times N}$, $D_s \in \mathbb{R}^{N\times N}$, and $c \in \mathbb{R}^{2\times N}$	Given matrices

$$y(k) = c\rho(k). \tag{6}$$

Table 1 summarizes the description of the PWSL model parameters. For more details related to the PWSL model, see [23].

To monitor traffic congestions, the PWSL model is constructed using only free-flow measurements (without considering the existence of wave congestion). The free PWSL model can be expressed by (7).

$$\rho(k+1) = A\rho(k) + Bu(k), \tag{7}$$

$$y(k) = c\rho(k). \tag{8}$$

The A and B matrices are described as follows:

$$A = \begin{bmatrix} 1 - z_1 v_{f,1} & 0 & 0 & \cdots & 0 \\ z_1 v_{f,1} & 1 - z_2 v_{f,2} & 0 & \ddots & \vdots \\ 0 & \ddots & \ddots & \ddots & 0 \\ \vdots & \ddots & & & 0 \\ 0 & \cdots & 0 & z_N v_{f,N-1} & z_N v_{f,N} \end{bmatrix}$$

$$B = \begin{bmatrix} z_1 & 0 & 0 & \cdots & 0 \\ 0 & \ddots & \ddots & \ddots & \vdots \\ \vdots & \ddots & z_{N-2} & 0 & \\ & & 0 & z_{N-1} & 0 \\ 0 & \cdots & & 0 & 0 \end{bmatrix}$$

where $z_i = \frac{\Delta T}{\Delta x_i}$.

3.2. Kalman filter for traffic density estimation

State estimation approaches or virtual sensing comes as an alternative solution for several reliability problems of embedded sensors [32,27,33,20]. In addition, in practice, unmeasurable variables (e.g., challenging and expensive to measure variables) can be estimated from other measurable variables using estimation methods. Furthermore, state estimation is used to monitor the state of sensors and their damaging positions. Kalman filter is one of the largely utilized estimation approaches in the literature of state estimation [32,34,27,35]. It is a linear state estimator that permits an optimal estimation in the presence of missing measurements and robust to measurement noise. In this paper, to further enhance traffic state estimation, the desirable properties of the PWSL model and Kalman filter are merged to create a PWSL Kalman filter (PWSL-KF)-based observer.

The correction terms and updating step constitute the essential components of PWSL-KF state prediction. Indeed, by minimizing the error covariance matrix, the estimated state vector can be generated and permits the generation of residuals that can be used in congestion detection. Considering the traffic system ((7), (6)), the PWSL-KF model evolved through the following steps:

- Correction terms

$$\hat{\rho}(k|k) = \hat{\rho}(k|k-1) + L(k)c(\rho(k|k-1) - \hat{\rho}(k|k-1)) \tag{9}$$

$$P(k|k) = (I - L(k)c)P(k|k-1) \tag{10}$$

$$L(k) = P(k|k-1)c^T\left[cP(k|k-1)c^T + R(k)\right]^{-1} \tag{11}$$

- Updating step

$$P(k|k-1) = AP(k-1|k-1)A^T + Q(k-1) \tag{12}$$

$$\hat{\rho}(k|k-1) = A\hat{\rho}(k-1|k-1) + Bu(k-1|k-1) \tag{13}$$

where $\hat{\rho}(k|k-1)$ and $\hat{\rho}(k|k)$ are the prior and the posterior density estimated, $P(k|k)$ is the estimation error covariance matrix, $Q(k-1)$ is the process noise covariance matrix and $R(k)$ is the measurement noise covariance matrix.

The estimation strategy is shown in Fig. 3. The Kalman filter receives as an input the information data about the input and output road section boundaries. By using this information the Kalman filter observer permits to estimate the dynamic of density in the considered road section.

4. *k*NN-based monitoring schemes

The k-nearest neighbors (kNN) is a very efficient nonparametric scheme to discriminate between different features [36,37]. Note that kNN is a flexible tool because it is assumption-free and no hypothesis is made on the data distribution. This property of kNN is very useful in particular when the data are non-Gaussian distributed or not linearly separable [38]. Overall, kNN separates normal data from abnormal data by measuring the distance between the actual observation and the k-nearest neighbors of anomaly-free (without congestion) data. Frequently, the Euclidean distance is used to measure the similarity in kNN–based approaches. In this study, kNN is applied to the residuals to check the presence of traffic congestions. kNN distances with large values are used as an indicator for discovering traffic congestions. Here, two methods using kNN distance are designed.

Essentially, kNN-based detectors are implemented in two stages without the need for any data labeling. At first, during the training stage, the detection limit of kNN, H, is calculated using free-flow data. Then, in the testing stage, the kNN distance between the new data and training data, D_{new}, is calculated and compared to the threshold H (Fig. 4).

4.1. Coupled kNN-Shewhart strategy

This approach combines kNN measures and Shewhart scheme [39]. In this approach, the Shewhart scheme is applied to kNN distance for detecting traffic congestion. In fact, for each residual of observation x_i in the training data, find its Manhattan and Euclidean distances to its nearest neighbor in the training data D_i, based on which sample distributions of distances can be computed;

$$D_i = \sum_{j=1}^{k} d_{ij}, \tag{14}$$

where d_{ij} is distance from observation to its j-th nearest neighbor. From the distribution of D_i, the parametric threshold of kNN-Shewhart approach is computed as:

$$H = \mu_D + 3\sigma_D, \tag{15}$$

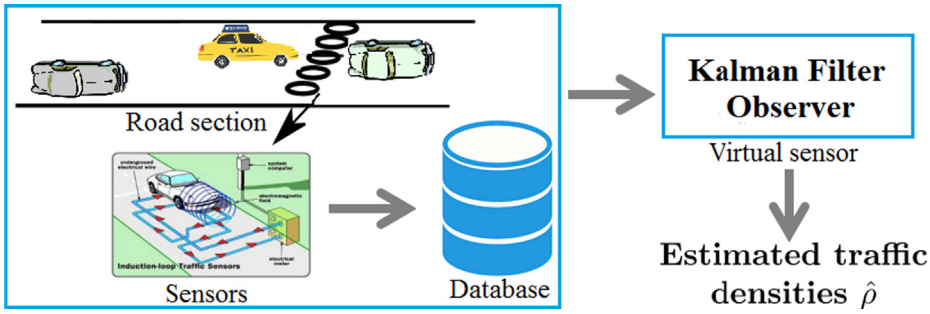

Fig. 3. Kalman filter-based estimation strategy.

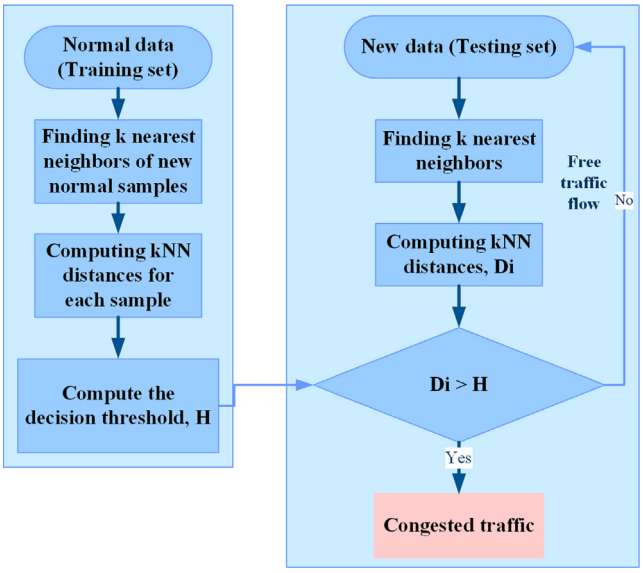

Fig. 4. Illustration of *k*NN procedure for detecting traffic congestion.

where μ_D and σ_D are the mean and standard deviation of *k*NN distances based on free-flow training data. Then, calculate Manhattan and Euclidean distance D_* for each residual of test data to its nearest neighbor in the training data. Congestions are uncover if D_* exceeds the threshold, H (Fig. 4).

4.2. Coupled kNN-ES strategy:

In this strategy, the *k*NN-exponential smoothing (ES) is utilized to evaluate the residuals produced by the PWSL-KF model. In this regard, *k*NN is employed for measuring the distance separating the current residual measurement and the normal training residual measurements. In the case of free-flow conditions, *k*NN distances fluctuate around to zero, while in the presence of congested conditions, large values of *k*NN distance can be obtained. The *k*NN-ES statistic is computed as:

$$z_{d_t} = v d_t + (1 - v) z_{d_{t-1}}, \tag{16}$$

where the initial value, z_{d_0} is the free-flow mean of the vector of *k*NN distances, μ_0^D. v $(0 < v1)$ is a smoothing parameter. Generally, small values of v are appropriate for the detection of small changes, while large values of v are suitable to detect large deviation [40,41]. The *k*NN-ES flags congestion if *k*NN-ES statistic surpasses the control limit, h, given as

$$h = \mu_0^{kNN} + L\sigma_0^{kNN}\sqrt{\left(\frac{v}{(2-v)}\left[1-(1-v)^{2t}\right]\right.}, \tag{17}$$

where L is the width of the control limit, $\sigma^{kNN} = \sigma_0^{kNN}\sqrt{\left(\frac{v}{(2-v)}\left[1-(1-v)^{2t}\right]\right.}$. The value of v defines the influence of the past observations on the actual observation [42].

4.3. kNN-based schemes using nonparametric control limits

The conventional parametric Shewhart and ES control procedures are suitable only when the normality assumption is valid. Indeed, the *k*NN algorithm is an efficient technique to identify the similarity between normal and abnormal features. However, associating it with a decision threshold based on the Gaussian distribution could degrade its performance. To bypass this limitation, the kernel density estimation [43] was used to estimate the distribution of *k*NN distances and compute a nonparametric threshold for traffic monitoring.

Step 1 Compute Manhattan or Euclidean distance, D_i, for each residual corresponding to the observation x_i in the training data to its nearest neighbor in the training data,

Step 2 From the distribution of D_i, a nonparametric threshold of *k*NN-Shewhart scheme is computed as the $(1-\alpha)$-th quantile of the estimated distribution of *k*NN distances obtained by kernel density estimation (KDE) (Fig. 5). Similarly, a nonparametric threshold of *k*NN-ES approach is defined as $(1-\alpha)$-th quantile of the estimated distribution of the *k*NN-ES statistic, z, obtained by KDE.

Step 3 Flag out traffic congestion when the kNN-based statistics (*k*NN-Shewhart or *k*NN-ES) exceed the control limit.

The threshold $h(\alpha)$ is selected to satisfy the following false alarm probability:

$$\mathbb{P}_1(z_t \geqslant h(\alpha)) = \int_h^{\infty} f_0(y)dy = 1 - \int_{-\infty}^{h} f_0(y)dy = \alpha \tag{18}$$

$$\int_{-\infty}^{h} f_0(y)dy = 1 - \alpha \tag{19}$$

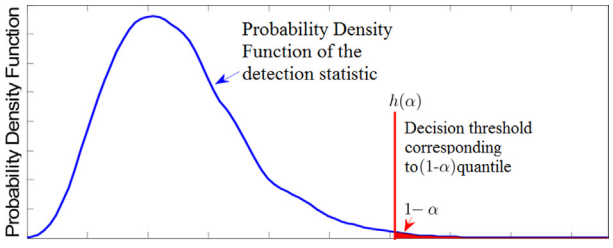

Fig. 5. Nonparametric computation of a decision threshold.

where $\mathbb{P}_1$ is probability distribution of the decision statistic (ES-KNN) with densities f_1 based on free-flow data. When the cumulative distribution function of a decision statistic is known, the q-quantiles are the application of the quantile function (the inverse function of the cumulative distribution function) to the values.

$$h(\alpha) = F^{-1}(1-\alpha). \tag{20}$$

where F^{-1} the inverse cumulative density function of the decision statistic based on free-flow data. When the normality assumption is invalid, the distribution of ES-KNN can be estimated by using the kernel density estimation. A nonparametric threshold of ES-KNN approach is defined as the $(1-\alpha)$ th quantile of the estimated distribution of ES-KNN obtained by KDE. We clarified that in the revised manuscript.

4.4. Compining PWSL-KF and kNN-ES for traffic monitoring

Here, the basic idea of the proposed *k*NN-based congestion detection methodology is briefly described. As described above, the use of the PWSL-KF observer is due to its simplicity and capability to appropriately estimate the unmeasured state. The PWSL-KF observer is designed based on uncongested traffic data and then adopted for monitoring new traffic data. Indeed, the PWSL-KF is used to generate residuals for congestion detection (Fig. 6). The residuals, $\mathbf{E} = [e_1, e_2, \ldots, e_n]$, are the difference between the real traffic density measurements, $\mathbf{Y} = [y_1, y_2, \ldots, y_n]$, and the output of the virtual sensor, $\hat{\mathbf{Y}} = [\hat{y}_1, \hat{y}_2, \ldots, \hat{y}_n]$, represented by the PWSL-KF observer.The residuals are defined as,

$$\mathbf{E} = \mathbf{Y} - \hat{\mathbf{Y}}. \tag{21}$$

The essence of the kNN-based charts is to measure the deviation separating the current residual and the residual of training data. In the absence of traffic congestion, kNN distance is fluctuating around zero, whereas in the presence of traffic congestions it diverges significantly from zero. Two strategies integrating the kNN and the exponential smoothing and Shewhart monitoring procedures were designed to monitor the PWSL-KF residuals. Specifically, these integrated strategies (with parametric and nonparametric thresholds) are employed to evaluate kNN distances for suitably identifying traffic congestions. If these kNN-based exponential smoothing and Shewhart thresholds are surpassed by the value of the decision functions, then it can be concluded that there is traffic congestion.

5. Results and case study

As mentioned above, in this paper we consider a road section of four cells from the State Route 60 (SR60) of California's highway. The calibration step plays a crucial role in the validation of macroscopic modeling approaches [23]. It permits to identify and estimate the model parameters through the approximation of the fundamental diagram (FD) schema. In this study, to feats the FD, we chose to use data of 98 days with a five minutes sample time for each vehicle detection station (VDS) of 99% detection functionality. This period is chosen for the aim to guarantee the existence of congestion data that permits the approximation of the second FD half.

The main concept of the calibration methodology used in this study is briefed here and more details can found in [44,23]. At first, a scatter plot of 98 days of bivariate data: traffic flow and traffic density (Fig. 7). From the scatter graph, the maximum value $\overline{Q}_{max}$ over all the flow points q_i can be obtained. Two regions can be discriminated by projecting $\overline{Q}_{max}$ on the axis of densities: traffic-free and congested regions. Then, we apply the first-order least-squares for data in each region and border the congestion line using two parallel lines that give the congestion direction. Hence, the critical density parameter ρ_c is obtained by taking the intersection between the upper line and the horizontal line according to $\overline{Q}_{max}$. The mean maximum flow of Q_{max} value can be estimated by the mean approximate values corresponding to the critical density. According to the Q_{max} value we fit both least-square lines, we can obtain the free flow speed v_f and the congestion wave speed, which are successively the slope values of the free and congestion lines. Finally, the jam density is obtained by the crossing point of the densities axis and congestion line. Of course, Fig. 7 displays the fundamental diagram parameters, which summarizes the calibration parameters.

By using this calibration methodology, we approximate the triangular form of the fundamental diagram for each cell. The calibrations results shown in Table 2.

To test the KF-PWSL observer we used two days data, the results are shown in Fig. 8.

Fig. 8 (a-d) display the estimation results of the SR60 road section for two days. These results illustrate the goodness of KF-PWSL observer for the estimation of traffic densities measurement. To assess the estimation accuracy, numerous statistical indices have been used in this study including root mean square error (RMSE), Coefficient of determination (r^2), and mean absolute percentage error (MAPE), these indices are defined as follows [45]:

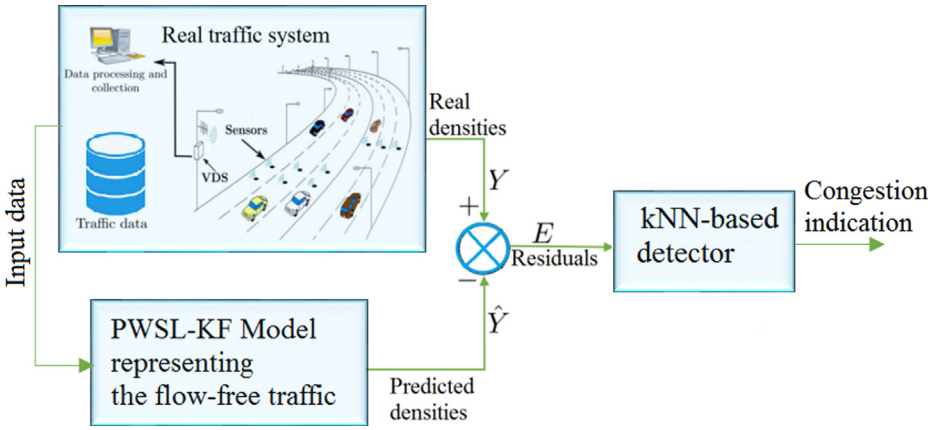

Fig. 6. PWSL-KF-based kNN methodology for traffic monitoring.

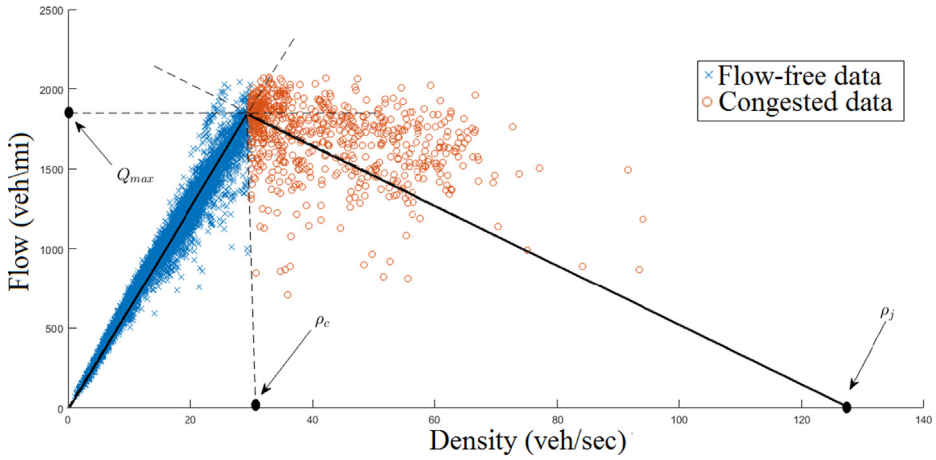

Fig. 7. The basic concept of identifying parameters in the fundamental diagram.

Table 2
Macroscopic parameters calibration of the SR60 road section.

Cells	v_f (mi/h)	w (mi/h)	ρ_c (vh/mi)	Q_M (vh/h)	ρ_{jam} (vh/mi)
1	64.1481	30.7717	25.8819	1557	84.1992
2	58.9681	26.4288	31.7438	1686	100.5007
3	62.4373	18.6045	30.7691	1664,5	130,4298
4	53.8030	18.6371	34,0653	1833	138,0098

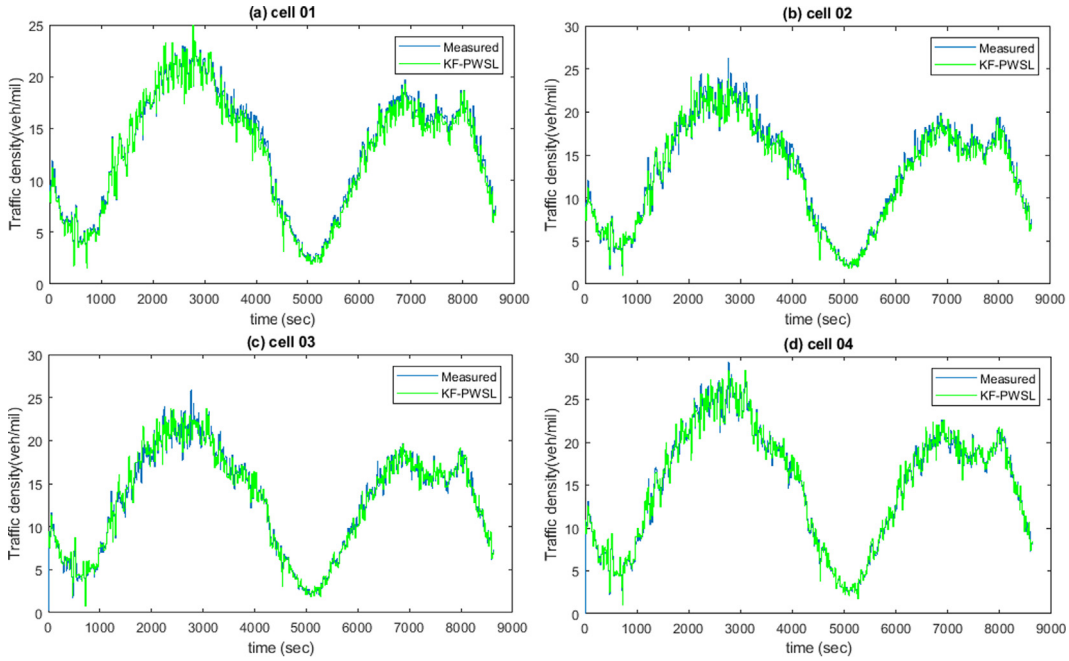

Fig. 8. Measured and KF-PWSL estimated densities, SR60 four cells, first day.

$$R^2 = 1 - \frac{\sum_{t=1}^{n}(y_t - \hat{y}_t)^2}{\sum_{t=1}^{n}(y_t - mean(Y))^2}, \tag{22}$$

$$RMSE = \sqrt{\frac{1}{n}\sum_{t=1}^{n}(y_t - \hat{y}_t)^2}, \tag{23}$$

$$MAPE = \frac{100}{n}\sum_{t=1}^{n}\left|\frac{y_t - \hat{y}_t}{y_t}\right|\%, \tag{24}$$

where y_t are the actual values, $\hat{y}_t$ are the corresponding estimated values by the KF-PWSL model and n is the number of measurements. Qualitatively, Table 3 shows the numerical metrics for error estimation, these results also prove the estimation quality of KF-PWSL.

5.1. Detection results

The detection ability of the kNN-based mechanisms to sense traffic congestions is checked. To quantify the detection quality

Table 3
KF-PWSL state estimation Metrics validation results.

Metrics	Cell 1	Cell 2	Cell 3	Cell 4
r^2	0.9937	0.9860	0.9825	0.9917
RMSE (vh/mi)	0.4541	0.6923	0.7740	0.6209
MAPE %	3.7294	4.7111	4.9130	3.4753

of our proposed monitoring approaches, we rely on a set of well-known anomaly detection performance metrics that are frequently used in the context of binary detection problems. In such type of a decision, a 2×2 confusion matrix, reporting the number of true positives (TP), false positives (FP), false negatives (FN), and true negatives (TN) is by convention used to summarize a detector's performance [46]. As a consequence, many common performance metrics are formed on the basis of this matrix. To assess quantitatively the detection efficiency of the proposed procedures, the following metrics will be used: true positive rate (TPR), false-positive rate (FPR), accuracy, and area under the curve (AUC). Fig. 9 illustrates a confusion matrix and summarizes equations of the main related metrics that are commonly used to assess the quality of a binary decision method and which will be used to assess the performance of the proposed PWSL-KF-based kNN congestion detection mechanisms.

5.1.1. Detection of abrupt congestions

Here, the feasibility of the PWSL-KF-based kNN mechanisms is verified to sense atypical abrupt changes in road traffic. The residuals, which are the mismatch between the output of the designed PWSL-KF observer and the measurements from the real sensors, are employed to flag out any deviation of the road traffic flow from the free-flow mode using kNN schemes. In other words, the statistical monitoring of the residuals with kNN-based detectors gives an indication of the presence of potential congestions. Two examples are presented to test the capability of the kNN-based congestion detectors in sensing abrupt congestions. First, to simulate abrupt congestion, a small bias of 10% of the total variation in the raw measurements is added in the raw measurements from sample ranges 2000 to 2500. In practice, this might be similar to congestion generated by a traffic jam during working hours. Fig. 10 displays the detection results of the kNN-based schemes. We can see that the four detectors signal the presence of traffic congestion (Fig. 10). Furthermore, the kNN-based Shewhart schemes (parametric and nonparametric) detect this congestion but with false alarms and missed detection.

Table 4 provides a summary of the detection quality of the four kNN-based detectors and the conventional ES and Shewhart charts. Here, the conventional charts are applied directly to the residuals obtained from the PWSL-KF model. Results in Table 4 highlight that the detection capability is improved by using the nonparametric k-NN-based approaches.

The testing data of the second example is contaminated with a bias of 20% of the total variation in the raw measurements from sample ranges 2000 to 2500. As expected, the four kNN-based procedure can sense this relatively large congestion (Fig. 11).

Table 5 summarizes the detection performance of the parametric and nonparametric kNN-Shewhart and kNN-ES mechanisms, and the conventional ES and Shewhart charts. kNN-Shewhart and kNN-ES procedures with nonparametric thresholds showed better detection performance compared to the parametric ones. Indeed, the nonparametric kNN-based procedures high accuracy (higher detection rate (TPR)) and precision (lower false alarms (FPR)). In

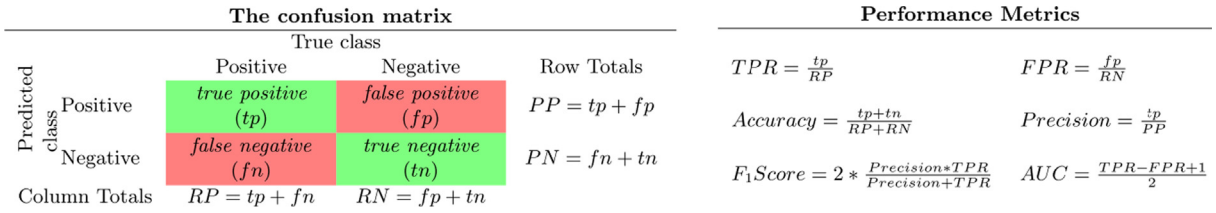

Fig. 9. Formulas of the usually used performance detection indices.

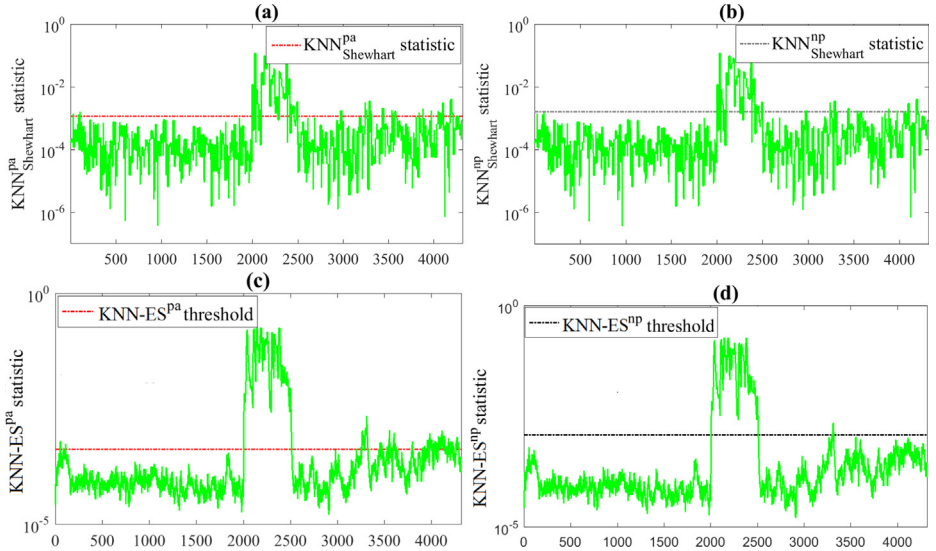

Fig. 10. Results from (a) KNN-Shewhart^{pa}, (b) KNN-Shewhart^{np}, (c) KNN-ES^{pa} and (d) KNN-ES^{np} detectors in the presence of an abrupt congestion (10% bias).

addition, the result highlights the superior performance of the nonparametric kNN-ES approach compared to the other approaches (Table 5).

Fig. 12 summarizes the AUC values of the six approaches for different congestion magnitudes. Fig. 12 indicates that nonparametric kNN-ES provides better detection efficiency compared to the other approaches in particular for congestion with a small magnitude. This is mainly due to the flexibility and efficiency of the PWSL-KF model to describe well the free-flow data and generating sensitive residuals and the good ability of the kNN-ES approach to uncover abnormal changes. In addition, these results indicate that applying kNN-based detectors results in improved detection accuracy than the use of the conventional charts (ES and Shewhart).

5.2. Scenarios with intermittent congestion:

The aim of this case is to evaluate the capability of the proposed methodologies in detecting intermittent congestions. Practically, intermittent congestions could be generated by several factors including traffic incidents and weather conditions. Here, a bias of amplitude 10% of the total variation of raw measurements is added to the testing measurements for samples 2000 to 2500, and for samples 3200 to 3400. The four monitoring procedures are displayed in Fig. 13(a-d). Fig. 13(a-d) indicates that the four schemes detect the introduced congestion. Table 6 illustrates the performance of parametric and nonparametric methods, and the conventional Shewhart and ES schemes. It can be seen that the Shewhart chart is inappropriate to apply in this case (Table 6). Essentially, this chart is designed based only on the current measurements and ignores the relevant information from past observations, which makes it insensitive to relatively small changes. An enhanced result is achieved when using the ES approach because this former used the actual and past data to uncover abnormal congestion. Table 6 highlights the superiority of the nonparametric kNN-based ES scheme with lower FPR and the highest TPR, accuracy, and precision. The AUC of the nonparametric kNN-ES scheme is 0.985. It should be also pointed out that the nonparametric kNN-Shewhart scheme and the parametric kNN-Shewhart and kNN-ES algorithms achieved respectively an AUC of 0.885, 0.873 and 0.946, they flag this abnormal congestion but with some false

Table 4
Detection indices by method when abrupt congestion has happened (10% bias).

Approach	TPR	FPR	Accuracy	Precision	F1 Score
KNN-ES^{np}	0.986	0.005	0.994	0.959	0.972
KNN-ES^{pa}	0.990	0.096	0.914	0.575	0.727
KNN-Shewhart^{np}	0.758	0.032	0.944	0.758	0.758
KNN-Shewhart^{pa}	0.816	0.048	0.936	0.690	0.748
Shewhart	0.531	0.027	0.921	0.7147	0.610
ES	1.000	0.203	0.820	0.392	0.564

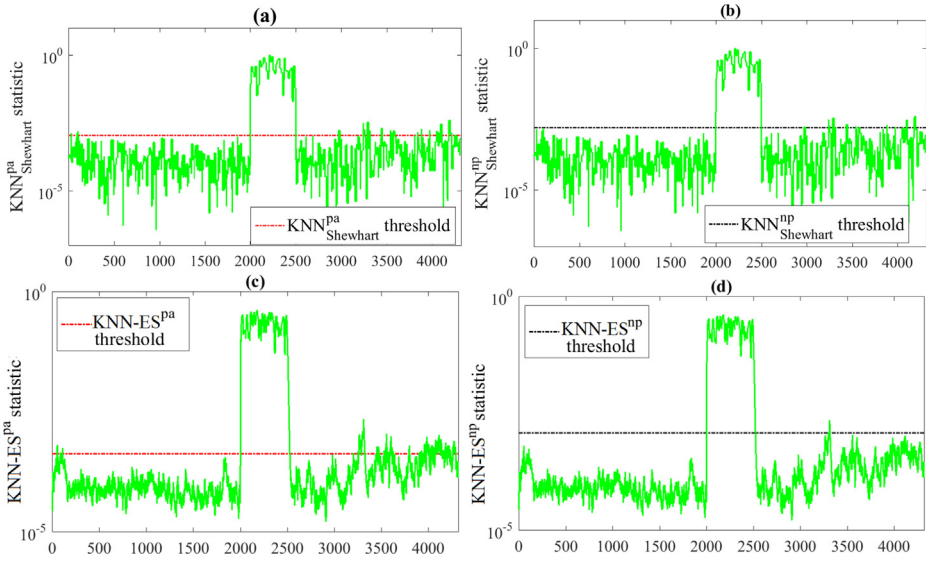

Fig. 11. Results from (a) KNN-Shewhart^{pa}, (b) KNN-Shewhart^{np}, (c) KNN-ES^{pa} and (d) KNN-ES^{np} detectors in the presence of an abrupt congestion (20% bias).

Table 5
Detection indices by method when abrupt congestion has happened (20% bias).

Approach	TPR	FPR	Accuracy	Precision	F1-Score
KNN-ES^{np}	0.992	0.009	0.991	0.938	0.964
KNN-ES^{pa}	0.992	0.100	0.911	0.567	0.721
KNN-Shewhart^{np}	1	0.032	0.972	0.805	0.892
KNN-Shewhart^{pa}	1	0.048	0.957	0.731	0.845
Shewhart	1	0.181	0.840	0.420	0.592
ES	1	0.060	0.947	0.686	0.814

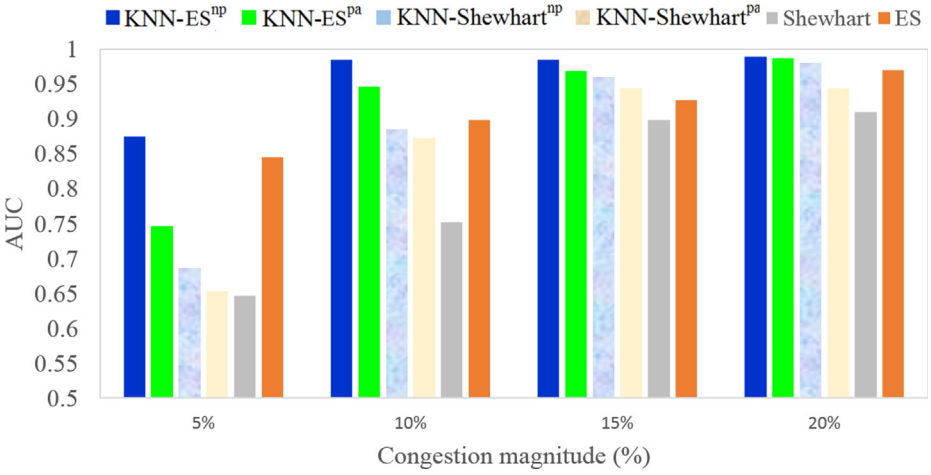

Fig. 12. AUC by method for different congestion magnitudes.

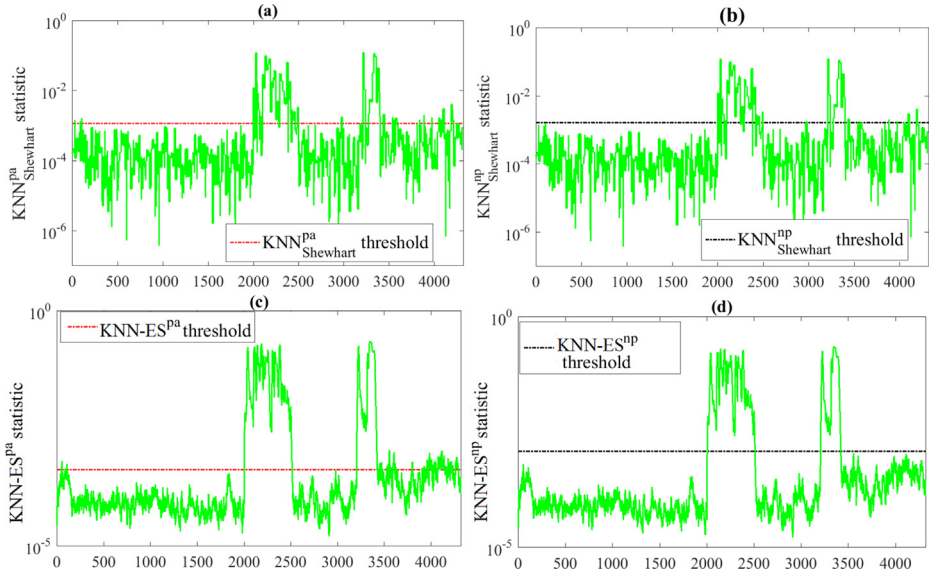

Fig. 13. Results from (a) KNN-Shewhart^{pa}, (b) KNN-Shewhart^{np}, (c) KNN-ES^{pa} and (d) KNN-ES^{np} detectors when an intermittent congestion has happened.

Table 6
Detection indices by method when intermittent congestion has happened.

Approach	TPR	FPR	Accuracy	Precision	F1 Score
KNN-ES^{np}	0.979	0.009	0.989	0.953	0.966
KNN-ES^{pa}	0.986	0.093	0.920	0.673	0.800
KNN-Shewhart^{np}	0.768	0.022	0.944	0.872	0.817
KNN-Shewhart^{pa}	0.811	0.039	0.936	0.800	0.805
Shewhart	0.997	0.265	0.778	0.422	0.593
ES	1	0.063	0.947	0.754	0.860

alarms and missed detection. As anticipated, the nonparametric kNN-ES scheme shows better performance compared to the other algorithms (Table 6).

5.3. Detection of gradual congestion:

The purpose of this scenario is to analyze the ability of the k-NN-based Shewhart and ES mechanisms (parametric and nonparametric) in detecting gradual congestions. A gradual congestion has been simulated by injecting in the raw traffic measurements a drifting with a slope of 0.01 from sample number 3000. Fig. 14 and Table 7 display the monitoring results of the four designed mechanisms. In addition, we compared the proposed schemes with conventional ES and Shewhart monitoring schemes (Table 7). Shewhart scheme achieved the lowest detection performance because it is based on the actual residual observation, which makes it insensitive to small changes. Results highlight the superior performance of the proposed nonparametric k-NN-based approaches. As nonparametric k-NN-based approaches are assumption-free give them the possibility of adapting it to a more complex situation compared to their parametric counterpart and conventional ES and Shewhart schemes.

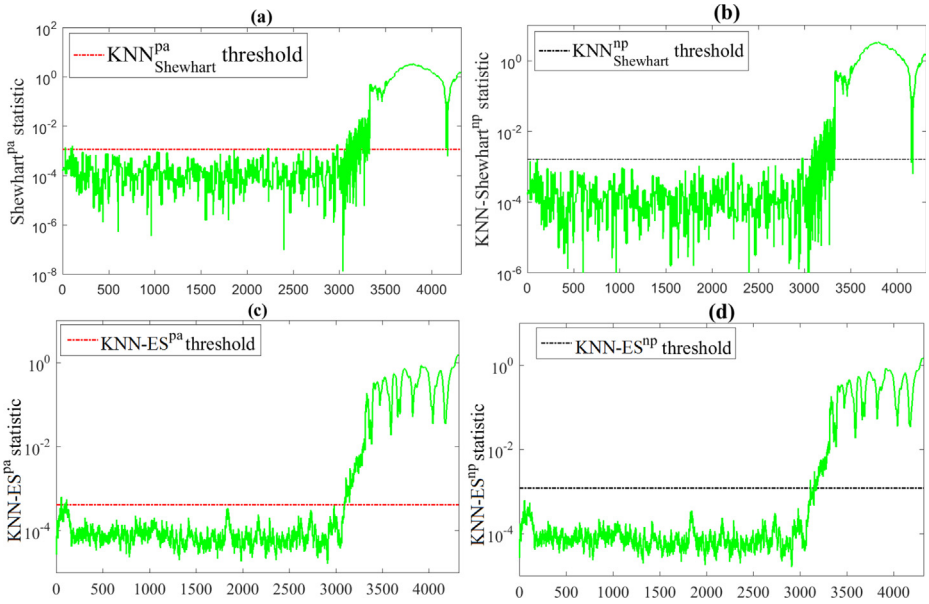

Fig. 14. Results from (a) KNN-Shewhart^{pa}, (b) KNN-Shewhart^{np}, (c) KNN-ES^{pa} and (d) KNN-ES^{np} detectors when a gradual congestion has happened.

Table 7
Detection indices by method for cases with gradual congestions.

Approach	TPR	FPR	Accuracy	Precision	F1 Score
KNN-ES^{np}	0.886	0	0.965	1	0.939
KNN-ES^{pa}	0.928	0.004	0.975	0.991	0.959
KNN-Shewhart^{np}	0.862	0.005	0.955	0.988	0.921
KNN-Shewhart^{pa}	0.878	0.010	0.956	0.974	0.924
Shewhart	0.965	0.130	0.899	0.766	0.854
ES	0.958	0.114	0.908	0.788	0.865

Overall, this work shows that the developed PWSL-KF-based kNN methodology has a good capability in identifying abrupt, intermittent and progressive congestions. Also, results proclaim the superior efficiency of the nonparametric kNN-based ES and Shewhart algorithms compared to the parametric ones. After comparing the kNN-Shewhart and kNN-ES schemes, results demonstrate that the kNN-ES mechanism exhibits suitable performance. This is mainly due to the fact that the kNN-ES incorporates all existing information from previous and actual observations in the decision, which extends its detection performance.

6. Conclusion

In this paper, the problem of traffic congestion detection is addressed. A hybrid observer merging the suitable characteristics of both the PWSL modeling and Kalman filter estimator is proposed to estimate the traffic density parameter. Moreover, an effective approach integrated the proposed PWLS-KF-based estimator and kNN-based detectors are designed to detect traffic congestions. Here, four kNN-based mechanisms have been introduced to detect traffic congestion, kNN- based Shewhart and exponential smoothing schemes (parametric and non-parametric). The feasibility of the proposed PWSL-KF-based kNN methodologies is assessed using measurements from the four-lanes SR-60 freeway in California. The results demonstrate that the proposed schemes are effective for detection of traffic congestions. Also, the analysis results highlight the superiority of the proposed method when using nonparametric thresholds computed via kernel density estimation, to the use of kNN parametric thresholds.

CRediT authorship contribution statement

Fouzi Harrou: Methodology, Formal analysis, Validation. **Abdelhafid Zeroual:** Data curation, Methodology, Validation. **Ying Sun:** Supervision, Conceptualization, Funding acquisition, Methodology.

Declaration of Competing Interest

The authors declare that they have no known competing financial interests or personal relationships that could have appeared to influence the work reported in this paper.

References

[1] S.C. Litescu, V. Viswanathan, H. Aydt, A. Knoll, The effect of information uncertainty in road transportation systems, J. Comput. Sci. 16 (2016) 170–176.
[2] M. Krbálek, J. Apeltauer, F. Šeba, Traffic flow merging-statistical and numerical modeling of microstructure, J. Computat. Sci. 32 (2019) 99–105.
[3] Y. Ji, X. Zhang, L. Sun, Estimation of traffic incident delay and its impact analysis based on cell transmission model, in Intelligent Vehicles Symposium (IV), 2011 IEEE. IEEE, 2011, pp. 54–59..
[4] T.-H. Chang, C.-H. Chueh, L.-K. Yang, Dynamic traffic prediction for insufficient data roadways via automatic control theories, Control Eng. Practice 19 (12) (2011) 1479–1489.
[5] A. Zeroual, F. Harrou, Y. Sun, N. Messai, Monitoring road traffic congestion using a macroscopic traffic model and a statistical monitoring scheme, Sustain. Cities Soc. 35 (2017) 494–510.
[6] N.K. Jain, R.K. Saini, P. Mittal, A review on traffic monitoring system techniques, in: K. Ray, T.K. Sharma, S. Rawat, R.K. Saini, A. Bandyopadhyay (Eds.), Soft Computing: Theories and Applications, Springer Singapore, Singapore, 2019, pp. 569–577.

[7] J. Barthélemy, N. Verstaevel, H. Forehead, P. Perez, Edge-computing video analytics for real-time traffic monitoring in a smart city, Sensors 19 (9) (2019), Available:https://www.mdpi.com/1424-8220/19/9/2048.
[8] M.S.R.S.T.M. Amir-Ul-Haque Bhuiyan, Mrinmoy Das, Computer vision based traffic monitoring and analyzing from on-road videos, Global J. Comput. Sci. Technol., 2019.
[9] M. Fernández-Sanjurjo, B. Bosquet, M. Mucientes, V.M. Brea, Real-time visual detection and tracking system for traffic monitoring, Eng. Appl. Artif. Intell. 85 (2019) 410–420.
[10] A. Dairi, F. Harrou, M. Senouci, Y. Sun, Unsupervised obstacle detection in driving environments using deep-learning-based stereovision, Rob. Autonomous Syst. 100 (2018) 287–301.
[11] A. Dairi, F. Harrou, Y. Sun, M. Senouci, Obstacle detection for intelligent transportation systems using deep stacked autoencoder and k-nearest neighbor scheme, IEEE Sens. J. 18 (12) (2018) 5122–5132.
[12] L. Jian, Z. Li, X. Yang, W. Wu, A. Ahmad, G. Jeon, Combining unmanned aerial vehicles with artificial-intelligence technology for traffic-congestion recognition: electronic eyes in the skies to spot clogged roads, IEEE Consumer Electron. Mag. 8 (3) (May 2019) 81–86.
[13] X. Li, H. Lu, City traffic flow character analysis and origin-destination estimation based on data mining, in: Information Computing and Telecommunications (YC-ICT), 2010 IEEE Youth Conference on, IEEE, 2010, pp. 142–145.
[14] F. Kong, J. Li, Z. Lv, Construction of intelligent traffic information recommendation system based on long short-term memory, J. Computat. Sci. 26 (2018) 78–86.
[15] Y.-J. Byon, A. Shalaby, B. Abdulhai, C.-S. Cho, H. Yeo, S. El-Tantawy, Traffic condition monitoring with scaat kalman filter-based data fusion in toronto, Canada, KSCE J. Civil Eng. 23 (2) (2019) 810–820, https://doi.org/10.1007/s12205-018-0132-5.
[16] W. Wang, J. Chen, Y.J. Wu, The prediction of freeway traffic conditions for logistics systems, IEEE Access 7 (2019) 13856–13861.
[17] P. Faldu, N. Doshi, R. Patel, Real time adaptive traffic control system: a hybrid approach, in: in 2019 IEEE 4th International Conference on Computer and Communication Systems (ICCCS), 2019, pp. 697–701.
[18] P.L. Juan Martín, Emil J. Khatib, R. Barco, Traffic monitoring via mobile device location, Sensors 19 (4505) (2019).
[19] F. Soriguera, F. Robusté, Estimation of traffic stream space mean speed from time aggregations of double loop detector data, Transp. Res. Part C: Emerging Technol. 19 (1) (2011) 115–129.
[20] A. Zeroual, F. Harrou, Y. Sun, N. Messai, Integrating model-based observer and kullback–leibler metric for estimating and detecting road traffic congestion, IEEE Sens. J. 18 (20) (2018) 8605–8616.
[21] Y. Wang, M. Papageorgiou, A. Messmer, Real-time freeway traffic state estimation based on extended kalman filter: adaptive capabilities and real data testing, Transp. Res. Part A: Policy Practice 42 (10) (2008) 1340–1358.
[22] Wenbin Zha, Yuqi Guo, Huawei Wu, Miguel Angel Sotelo, Yulin Ma, Qian Yi, Zhixiong Li, Xin Sun, A new switched state jump observer for traffic density estimation in expressways based on hybrid-dynamic-traffic-network-model, Sensors 19 (3822) (2019).
[23] A. Zeroual, N. Messai, S. Kechida, F. Hamdi, A piecewise switched linear approach for traffic flow modeling, Int. J. Autom. Comput. (2017).
[24] D. Simon, Optimal State Estimation, C.S. University, Ed. John Wiley & Sons, Inc., Publication, 2006..
[25] D. Jwo, S. Wang, Adaptive fuzzy strong tracking extended kalman filtering for gps navigation, IEEE Sens. J. 7 (5) (May 2007) 778–789.
[26] S. Wang, C. Wang, M. Chang, C. Tsai, C. Chang, Applications of kalman filtering to single hyperspectral signature analysis, IEEE Sens. J. 10 (3) (March 2010) 547–563.
[27] G. Rigatos, D. Serpanos, N. Zervos, Detection of attacks against power grid sensors using kalman filter and statistical decision making, IEEE Sens. J. 17 (23) (Dec 2017) 7641–7648.
[28] A. Assa, F. Janabi-Sharifi, A kalman filter-based framework for enhanced sensor fusion, IEEE Sens. J. 15 (6) (June 2015) 3281–3292.
[29] P.H.R.P.J. Lu, Xiao-Yun Varaiya, Faulty loop data analysis/correction and loop fault detection, in 15th World Congress on Intelligent Transport Systems and ITS America's 2008 Annual Meeting, 2008..
[30] C.F. Daganzo, The cell transmission model, part II: Network traffic, Transp. Res. Part B: Methodol. 29 (2) (1995) 79–93.
[31] M.J. Lighthill, G.B. Whitham, On kinematic waves. II. A theory of traffic flow on long crowded roads, Proc. R. Soc. A: Math., Phys. Eng. Sci. 229 (1178) (1955) 317–345.
[32] T. Seo, A.M. Bayen, T. Kusakabe, Y. Asakura, Traffic state estimation on highway: a comprehensive survey, Annu. Rev. Control 43 (2017) 128–151.
[33] Z. Li, K. Goebel, D. Wu, Degradation modeling and remaining useful life prediction of aircraft engines using ensemble learning, J. Eng. Gas Turbines Power 141 (4) (2019) 041008.
[34] M. Weiss, M.S. Wiederoder, R.C. Paffenroth, E.C. Nallon, C.J. Bright, V.P. Schnee, S. McGraw, M. Polcha, J.R. Uzarski, Applications of the kalman filter to chemical sensors for downstream machine learning, IEEE Sens. J. 18 (13) (2017) 5455–5463.
[35] A. Baghdadi, L.A. Cavuoto, J.L. Crassidis, Hip and trunk kinematics estimation in gait through kalman filter using imu data at the ankle, IEEE Sens. J. 18 (10) (2018) 4253–4260.
[36] J. Han, J. Pei, M. Kamber, Data mining: Concepts and Techniques, Elsevier, 2011.
[37] T. Cheng, F. Harrou, Y. Sun, T.O. Leiknes, Monitoring influent measurements at water resource recovery facility using data-driven soft sensor approach, IEEE Sens. J. 19 (1) (2018) 1–11.
[38] X. Wu, V. Kumar, J.R. Quinlan, J. Ghosh, Q. Yang, H. Motoda, G.J. McLachlan, A. Ng, B. Liu, S.Y. Philip, et al., Top 10 algorithms in data mining, Knowledge Inf. Syst. 14 (1) (2008) 1–37.
[39] F. Kadri, F. Harrou, S. Chaabane, Y. Sun, C. Tahon, Seasonal ARMA-based SPC charts for anomaly detection: application to emergency department systems, Neurocomputing 173 (2016) 2102–2114.
[40] D. Montgomery, Introduction to Statistical Quality Control, John Wiley & Sons, 2007.
[41] F. Harrou, Y. Sun, M. Madakyaru, B. Bouyedou, An improved multivariate chart using partial least squares with continuous ranked probability score, IEEE Sens. J. 18 (16) (2018) 6715–6726.
[42] F. Harrou, M.N. Nounou, Monitoring linear antenna arrays using an exponentially weighted moving average-based fault detection scheme, Systems Sci. Control Eng.: Open Access J. 2 (1) (2014) 433–443.
[43] E. Martin, A. Morris, Non-parametric confidence bounds for process performance monitoring charts, J. Process Control 6 (6) (1996) 349–358.
[44] A. Zeroual, N. Messai, S. Kechida, and F. Hamdi, Calibration and Validation of a Switched Linear Macroscopic Traffic Model, in 3rd International Conference on Control, Engineering & Information Technology CEIT2015, no. 1. IEEE, 2015, pp. 25–27..
[45] Z. Li, D. Wu, T. Yu, Prediction of material removal rate for chemical mechanical planarization using decision tree-based ensemble learning, J. Manuf. Sci. Eng. 141 (3) (2019) 031003.
[46] D.M. Powers, Evaluation: from precision, recall and f-measure to ROC, informedness, markedness and correlation, 2011..